

Khan, Z., Yusup, S., Ahmad, M. M., Inayat, A., Naqvi, M., Sheikh, R. and Watson, I. (2018) Integrated catalytic adsorption steam gasification in a bubbling fluidized bed for enhanced H₂ production: perspective of design and pilot plant experiences. *Biofuels, Bioproducts and Biorefining*, 12(5), pp. 735-748.

There may be differences between this version and the published version. You are advised to consult the publisher's version if you wish to cite from it.

Khan, Z., Yusup, S., Ahmad, M. M., Inayat, A., Naqvi, M., Sheikh, R. and Watson, I. (2018) Integrated catalytic adsorption steam gasification in a bubbling fluidized bed for enhanced H₂ production: perspective of design and pilot plant experiences. *Biofuels, Bioproducts and Biorefining*, 12(5), pp. 735-748. (doi:[10.1002/bbb.1885](https://doi.org/10.1002/bbb.1885))

This article may be used for non-commercial purposes in accordance with [Wiley Terms and Conditions for Self-Archiving](#).

<http://eprints.gla.ac.uk/162575/>

Deposited on: 09 July 2018

Integrated catalytic adsorption steam gasification in a bubbling fluidized bed for enhanced H₂ production: Perspective of design and pilot plant experiences

Zakir Khan^{1,2,*}, Suzana Yusup³, Murni M Ahmad^{3†}, Abrar Inayat⁴, Muhammad Naqvi⁵, Rizwan Sheikh⁶, Ian Watson²

¹Department of Chemical Engineering, COMSATS University Islamabad, Lahore Campus, 54000, Pakistan

²Systems Power and Energy, School of Engineering, University of Glasgow, Glasgow, G12 8QQ, UK

³Centre for Biofuel and Biochemical, Universiti Teknologi PETRONAS, Bandar Seri Iskandar, Tronoh, 31750, Perak, Malaysia

⁴Department of Sustainable and Renewable Energy Engineering, University of Sharjah, Sharjah, 27272, United Arab Emirates

⁵Future Energy Center, School of Business, Society and Engineering, Mälardalens University, Västerås, Sweden

⁶NFC IET, PO Opposite Pak Arab Fertilizers, Khanewal Road, Multan, Pakistan.

ABSTRACT

It is important to build knowledge on the design of an integrated catalytic adsorption (ICA) steam gasification process in a bubbling fluidized bed to reduce CO₂ content with enhanced hydrogen production. The news value of this study is presentation of detailed design considerations for performance evaluation of ICA system utilizing palm oil wastes as feedstock. The main advantage of utilizing ICA gasification system is the CO₂ adsorption through carbonation reaction (using CaO) that help water gas shift reaction to move forward. Whereas the catalyst activity improves steam methane reforming in parallel which not only produces additional hydrogen but also releases CO to enhance the activity of water gas shift reaction. The performance of the developed system has shown least temperature variation (< 1%) inside reactor which inferred the positive role of exothermic reactions between reactive bed material (CaO) and CO₂ in the product gas. The low-pressure drop in the gasifier (100-130 mbar) further strengthens the presented design strategy for ICA gasification system for hydrogen production. Further, the challenges encountered during the pilot plant operations and their potential solutions have been discussed to improve and optimize the operation, especially for downstream equipment and auxiliaries.

*Corresponding author: [Tel:+92 111-001-007](tel:+92111-001-007) ext. 884

E-mail address: zkhan@ciitlhore.edu.pk, zakir.khan@glasgow.ac.uk

Keywords: Fluidized bed, integrated catalytic adsorption, hydrogen, palm kernel shell, steam gasification

1. Introduction

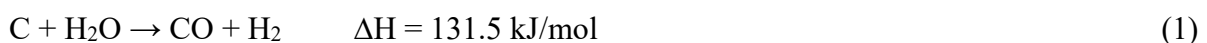
Concerted efforts have been made to develop advance biomass gasification technologies in the last couple of decades. Present biomass gasification technologies are based on coal gasification processes but with slight modification due to the high volatile matter and low temperature of operation. These technologies mainly comprised of a fixed bed, fluidized bed entrained flow reactors, plasma reactors and rotary kiln reactors ¹. However, fixed bed, fluidized bed and entrained flow gasifiers are mostly utilized for hydrogen production from biomass gasification ². Fluidized bed (FB) gasifiers have proven to be the efficient for combustion and gasification processes due to their high mass and heat transfer capability. The FB gasifiers are considered to be an effective choice for biomass gasification as they accept a wide variety of biomass, produce high carbon conversion rates and provide uniform temperature distribution in the gasifier ³. These types of gasifiers accept small feed size compared to the fixed bed gasifiers, and they are capable of handling higher and lower quality fuels ⁴.

Recent application of catalyst and *in situ* CO₂ adsorption to enhance hydrogen from biomass gasification makes the process more viable for commercial scale. Udomsirichakorn and Salam ⁵ review biomass steam gasification technologies utilizing *in situ* CO₂ adsorption techniques to produce hydrogen. Most of these studies ⁵ comprise fixed and fluidized beds including a dual fluidized bed reactor. Many researchers ⁶⁻⁸ have developed the concept of gasification via chemical looping for hydrogen production utilizing CaO as an adsorbent which implied regeneration of the adsorbent in a different reactor. More recently, the development of fluidized bed gasifier and sorption-enhanced reforming process (SERP) has been proposed for biomass steam gasification to enhance hydrogen production ⁹. This system has worked on gasification

followed by SERP contains a mixture of Ni-based catalyst and CaO sorbent. New developments demonstrate the tremendous efforts that are being made to enhance the quality and quantity of renewable hydrogen from biomass gasification. The efforts are mainly focused on reducing the number of process units by introducing novel catalyst^{10, 11}, CO₂ sorption⁶⁻⁸ or coupling of both in the same reactors (after gasification step)⁹ and/or in separate reactors (after the pyrolysis step)¹². Therefore, development of a single gasifier utilizing catalyst and CO₂ adsorbent in the same bed will be worthwhile to investigate.

Based on our previous research work, there are advantages of the process to operate in a single unit in order to minimize the capital cost by avoiding additional downstream units^{13, 14}. Secondly, the benefits of utilizing methane reforming catalyst and CO₂ sorbent together in one bed and a single reactor can be understood by considering the main biomass steam gasification reactions with in-situ CO₂ adsorbent (Equations 1-4). The capturing of CO₂ takes place via carbonation reaction (Eq. 4) accelerates the water gas shift reaction towards enhanced hydrogen production under Le Chatelier's principle. The amounts of CO react in water gas shift (Eq. 3) comes from steam methane reforming (Eq. 2) and char gasification (Eq. 1), and provides an opportunity to accelerate the former reaction through the enhanced activity of later reactions. Steam methane reforming and char gasification are both endothermic reactions and the activities are heavily depending on the high temperature. However, temperature > 725°C for biomass gasification with in-situ CO₂ adsorbent in the bed is a matter of concern due to reverse carbonation especially when CaO is used as an adsorbent¹⁵⁻¹⁸. Therefore, using steam methane reforming catalyst in the bed not only enhance hydrogen production but also provide more CO (even at low temperature) to allow the water shift reaction to move in a forward direction.

Char gasification reaction (CGR),



Steam methane reforming (SMR),



Water gas shift reaction (WGSR),



Carbonation reaction



The present study is a continuation of our research work to develop integrated catalytic adsorbent (ICA) steam gasification using the bubbling fluidized bed. A part of ICA steam gasification process evaluates the optimum process conditions for hydrogen production, has been published ^{13, 14, 19} whereas detail process and design development, and operational challenges of this pilot scale study are not reported yet. The news value of this study is the design considerations and pilot plant experiences of a bubbling fluidized bed gasification system for enhanced H₂ production that utilizes a catalyst (Ni-based) and adsorbent (CaO) in a single bed inside the reactor. The design strategy is carried out by combining the reactor hydrodynamics and reaction based steam required for the gasification reactions. A number of parameters e.g. minimum fluidization velocity, transport disengaging height, maximum bubble diameter, bed to distributor plate pressure drop ratio are investigated to evaluate reactor dimensions and distributor plate design. The performance of the developed pilot scale ICA gasification system is carried out through temperature pressure profiles and velocity-pressure diagrams to ensure sufficient fluidization conditions in the bed. The issues encountered during the system operation and the potential solutions have been discussed to improve and optimize the operation, especially for downstream equipment and auxiliaries. The impact of vital performance parameters, such as product gas composition, hydrogen yield and gas heating

values are further discussed. The study is intended to assist the scientific community, companies, governmental energy agencies and relevant stakeholders to further develop efficient ICA steam gasification process for enhanced H₂ production.

2. Methodology and key design parameters

2.1 ICA steam gasification system

Fig. 1 shows a process diagram of pilot scale fluidized bed ICA steam gasification system. The gasification system mainly comprises of fluidized bed reactor with external electric heaters, biomass feeding system, steam generator and superheater, cyclone solid separator, wet scrubber, water separator, and gas analyzing the system. After the gasifier, product gas passes through the cyclone to separate solid particles from the product gas. The product gas then passes through the scrubber and attains a temperature less than 40 °C and then followed by a separator to remove any final traces of water in the product gas stream. The gas sampling point is located at the exit of the water separator. The gas analysing system consists of Gas Chromatography (Teledyne 7500, Teledyne Analytical Instrument) with Infrared (IR) type detector. Hydrogen and nitrogen are detected by Gas Chromatography utilizing Molecular Sieve 5A column (Teledyne 4060, Teledyne Analytical Instrument) with Thermal Conductive Detector (TCD). The product gas is measured every 6 minutes at the sampling point located after the water separator.

ICA gasification system is developed to operate at a temperature range of 600-750 °C, under atmospheric pressure. This temperature range provides an active carbonation region when CaO is used as a bed material to adsorb CO₂²⁰.

2.2 Materials and gasification agent

Palm kernel shell (PKS) is selected as the feedstock for hydrogen production via ICA steam gasification. It is estimated that a total of 12.8 Mt of PKS are generated in 2015 by Malaysia and Indonesia ^{21, 22} which are the largest oil palm producers in the world ²³ . Based on its abundance and physical properties i.e. high proportion of fixed carbon, volatile matter, and low ash and moisture content, PKS has the potential to enhance hydrogen production via gasification ²⁴. The ultimate analysis of PKS has performed in LECO CHNS 932 elemental analyser. A standard sample of approximately 2 mg was put in the silver capsule and analysed. The furnace temperature was maintained at 1000°C. The proximate analysis (volatile matter, ash content, and fixed carbon) was determined based on a dry basis. For ash content, ASTM D-3175-01 procedure was used to evaluate the ash content in the biomass. The sample was then cooled and weighed. The volatile matter was determined by following ASTM E-872 procedure. Fixed carbon was determined by subtracting the sum of volatiles matter and ash content in the biomass based on the dry basis. The calorific value of PKS was determined in IKA C5000 oxygen bomb calorimeter. The ASTM E711-87 procedure was considered to determine the calorific value. The physical properties of PKS are listed in Table 1.

The present work proposes *in situ* CO₂ adsorption and emphasis on the reactive bed particle which can provide smooth fluidization as well as effective CO₂ absorption in the bed. Naturally occurring metal oxides (MO), abundant in natural rocks, are proved to be low-cost CO₂ adsorbent material ²⁵ through the following reaction.



However, decomposition temperature (calcination temperature) of these metal carbonates (MCO₃) i.e. MgCO₃ (385°C), ZnCO₃ (340°C) and MnCO₃ (440°C) is low which makes them unsuitable for *in situ* CO₂ capture in biomass gasification ²⁶. Among these metal oxides, the decomposition temperature for CaCO₃ is 800°C which makes CaO more suitable as a sorbent ²⁷. Besides, CaO can also be extracted from different sources i.e. eggshell ²⁸ and cockle shell

²⁹ in the form of CaCO_3 which is further calcined and used as a CaO for CO_2 adsorption. In the present study, Quicklime (CaO) is used as the bed particle to adsorb CO_2 at the gasification temperature. The quicklime was purchased from Universal Lime Sdn. Bhd., Malaysia. The main source of the quicklime is natural occurring limestone which is abundant in the local area of Perak, Malaysia. The physical properties and chemical composition ³⁰ is shown in Table 2. Based on their properties, these materials are well represented by the Geldart particle B (sand like) which represents good fluidization characteristics to achieve better heat and mass transfer rates to keep homogeneous temperature all over the bed.

Steam as an oxidizing agent has gained a high reputation due to the resulting hydrogen-rich gas production ²⁶. The properties of steam for the case are given in Table 2. Steam gasification produces 5 times more hydrogen content than air gasification in fluidized bed gasifier ³¹ and thus considered as the gasification medium in the present study.

Nickel (Ni) is the most widely used catalyst in steam and dry reforming processes. There is a significant body of work reported on the application of Ni catalysts in biomass gasification ^{32, 33}. In the present study, purified Ni powder with 99.5 % purity and average particle size of 10 μm is used. The Ni catalyst is purchased from Merck KGaA, Germany. Throughout the ICA gasification runs, Ni catalyst is mixed with palm kernel shell (PKS) at a fixed ratio of 0.1 (wt./wt.) and introduced to the gasifier via the biomass feeding system.

2.3 Reactor diameter evaluation

Fluidized bed gasifier design initially considers the evaluation of the gasifier diameter. Steam as a gasification agent also has an additional role of fluidizing the bed. This dual role needs to be balanced. Fig. 2 shows the diameter estimation process through the combination of minimum fluidization velocity (U_{mf}) as a hydrodynamics parameter and total steam requirement as a reactant for the gasification reactions. The present study considers that the

bubbling fluidized bed is characterized by a superficial gas velocity (U) of the order of a U_{mf} ³⁴. Similarly, the total steam required for U_{mf} is a few orders of steam required for gasification reaction. The evaluation of U_{mf} is based on the physical properties of the bed particles and steam. These properties include average particle diameter, particle density, bulk density, and steam density and viscosity. The density and viscosity of steam are considered at the fluidization conditions of 750 °C and 1 atm^{35,36} (Table 2).

The minimum fluidization velocity (U_{mf}) is a basic design parameter to define fluidization conditions in the bed. The modified form of Ergun's equation in the form of Archimedes number (Ar) for the pressure drop across a fixed bed at minimum fluidization conditions is used to estimate U_{mf} ³⁷ and given by Equation (6):

$$Ar = 150 \left(\frac{1 - \varepsilon_{mf}}{\varphi_b^2 (\varepsilon_{mf}^3)} \right) Re_{mf} + \left(\frac{1.75}{\varphi_b^2 (\varepsilon_{mf}^3)} \right) Re_{mf}^2 \quad (6)$$

Where Ar can be calculated as:

$$Ar = d_b^3 \rho_f \left(\frac{\rho_p - \rho_f}{\mu^2} \right) g \quad (7)$$

The Reynolds number at the minimum fluidization condition is:

$$Re_{mf} = \frac{d_p \rho_f U_{mf}}{\mu} \quad (8)$$

Where d_b and ρ_b are the bed particle diameter (m) and density (kg/m³), respectively, ρ_f and μ are the viscosity (Pa. s) and density (kg/m³) of steam, g is the acceleration due to gravity (m/s²), ε_{mf} is the bed voidage at the minimum fluidization velocity and φ_b is the bed particle sphericity.

Bed voidage and sphericity must be known at minimum fluidization to estimate U_{mf} using

Equations (6), (7) and (8). These basic equations give more reliable predictions of U_{mf} as compared to empirical expressions³⁷ and thus they are used herein. ε_{mf} is calculated from the following expression³⁸:

$$\varepsilon_{mf} = \frac{\rho_b}{\rho_p} - 1 \quad (9)$$

The sphericity for CaO is calculated from previously published work³⁹ using Equations (6)-(8) for known minimum fluidization velocity. The sphericity determined value is 0.43 which is in a good agreement with the value reported by Basu⁴⁰.

The steam, needed for the gasification reactions as the reactant is evaluated. These main reactions are char gasification, methane steam reforming and the water gas shift as represented by Equations (1- 4):

The total amount of steam required (S_{total}) for gasification is given by:

$$S_{Total} = S_{CGR} + S_{SMR} + S_{WGSR} \quad (10)$$

The following scheme is considered to calculate the amount of steam required for each of the reactions involved:

- CGR: Char is produced according to the fixed carbon content of biomass from the proximate analysis⁴¹. This char is expected to participate in the CGR and thus can be estimated directly from the given biomass feed rate.
- SMR: The biomass devolatilization produces gases such as H₂, CO, CO₂, CH₄ and H₂O⁴². The amount of CH₄, released from biomass, is estimated based on the proximate and ultimate analysis. The total elemental carbon content in biomass is 49.74 wt% which consists of fixed carbon (C) and volatile matter (assumed to be CH₄ only). The remaining carbon portion in the volatile matter is estimated by subtracting the fixed carbon from the total elemental carbon.

- WGSR: The amount of steam available for the water gas shift reaction is estimated from CO produced by char gasification and steam methane reforming reactions. The amount of CO in the water gas shift reaction is considered as the sum of the CO generated from char gasification and steam methane reforming reactions.

2.4 Gasifier Height

The height of the fluidized bed reactor is calculated based on the transport disengaging height (TDH) [24], the height over which only fine particles are carried over, and the bed height (Fig. 3)³⁷. The equation of reactor height can be written as:

$$\text{Reactor height} = \text{TDH} + \text{Bed height} \quad (11)$$

Above the TDH, the rate of carryover of fine particles is constant. Moreover, the height of which gas exits from the fluidized bed reactor should be higher than TDH to minimize the entrainment of solid particles.

Several empirical expressions are used to determine the TDH based on the maximum bubble diameter. Among these, Horio's empirical equation and Zenz's graphical presentation are more reliable³⁸. However, the graphical presentations are only available for fine particles corresponding to Geldart particles A³⁷; whereas the present study considered Geldart particles B. The equation presented by Horio³⁸ for TDH is considered in the present case which can be used for Geldart particles B:

$$\text{TDH} = 4.47(D_{bm})^{0.5} \quad (12)$$

Where D_{bm} is the maximum bubble diameter on the surface of the bed.

The maximum bubble diameter (D_{bm}) is an important parameter to avoid slugging in bubbling fluidized bed reactors. The mass transfer rate between the bubble and emulsion phases is an important parameter that influences the overall reaction rate.

In the present study, Mori and Wen's correlation, ⁴³ is used to determine the D_{bm} . This correlation is valid for both Geldart types B and D particle classification:

$$D_{bm} = 0.652 \left[A(U - U_{mf}) \right]^{2/5} \quad (13)$$

Where U is the superficial gas (steam) velocity (m/s) and A is the bed cross-sectional area (m²). Maximum bubble diameter increases with increasing superficial velocity and bed height ^{40, 44}. For better fluidization conditions in the bed, it is generally recommended that the ratio of bed height (Z) to bed diameter (D) needs to be ≤ 2.0 to avoid slugging ⁴⁵. Slugging occurs when the bubble reaches the size of the bed diameter. At this stage, the bubble passes through the bed as a slug and fluidization conditions are not sustained in the reactor ³⁸. In the present study, a ratio of 1.0 is considered to facilitate a good fluidization region and also to keep the bubble size sufficiently small to avoid slugging.

2.5 Distributor plate design

The distributor plate plays a vital role in generating homogeneous fluidization conditions all over the bed. It is important that the fluidized bed distributor is properly designed to ensure uniform distribution of gas flow. Better design approaches of distributor plates for good fluidization depends on a certain ratio between the pressure drop across the distributor plate and bed. A perforated plate type distributor is used due to its fabrication simplicity, hole size modification and ability to be cleaned easily

Zuiderweg et al.³⁷ used a rule of thumb to obtain the pressure drop across the distributor plate. They considered 0.2-0.4 ratio for the distributor pressure to the bed pressure drop. However, this approach gives a high-pressure drop inside the reactor³⁷ and is not considered in the present study. Qureshi et al.⁴⁶ developed an empirical relationship for the ratio of distributor pressure to bed pressure drop (R_c), and showed stable and unstable operational regions of the distributor using the following expression:

$$R_c = 0.01 + 0.02 \left(1 - \exp \left(\frac{-0.5D}{Z} \right) \right) \quad (14)$$

Where D is the bed diameter (m) and Z is the bed height (m). The aspect ratio of the bed (D/Z) is assumed as 1.0 to ensure a stable operating region for the distributor⁴⁶. The pressure drop across the bed at superficial velocity (5 times of U_{mf} in the present study) is then calculated from Equation (14)³⁷.

$$\Delta P_b = Z(1 - \varepsilon)(\rho_p - \rho_f) \quad (15)$$

Where ε refers to bed voidage and Z is the bed height at the superficial gas velocity. Bed voidage at superficial velocity can be considered equal to the bed voidage at minimum fluidization ($\varepsilon = \varepsilon_{mf}$) because no change in pressure drop can be seen for Geldart B type particles, if the gas velocity rises over the minimum fluidization velocity³⁸. The distributor pressure drop is determined using Equation (13) which is further used to determine the total number of orifices needed in the perforated distributor plate (Table 3).

A general design procedure for estimating the total number of orifices on a triangular pitch³⁷ is followed:

- Number of orifice (N_{or}) in the distribution plate is determined using the following expression:

$$N_{or} = A_{or} \left(\frac{U_{or}}{Q_{mf}} \right) \quad (16)$$

Q_{mf} , A_{or} , U_{or} are the minimum fluidization volumetric flow rate (m^3/h), area of each orifice (m^2) and gas velocity (m/s) through the orifice in the distributor plate respectively. All of these quantities are dependent on the properties of the fluidizing agent (density and viscosity of steam).

- The gas velocity through the orifices is calculated using:

$$U_{or} = C_{dor} \left(\frac{2\Delta P_d}{\rho_f} \right) \quad (17)$$

Where ΔP_d is the pressure drop (bar) across the distributor plate. This is calculated based on the pressure in the bed as $\Delta P_d = 0.089 \Delta P_b$, where 0.089 represents R_c (Equation 14). Constant, C_{dor} , is the drag coefficient.

- The drag coefficient, C_{dor} (dimensionless), and Vessel Reynolds number ($R_{e(v)}$) based on the diameter of the vessel (reactor) are related as follows:

$$R_{e(v)} = \rho_f \left(\frac{U_{or} D}{\mu} \right) \quad (18)$$

The total number of orifices in the distributor plate is then evaluated.

3. Results and Discussions

3.1 Fluidized bed gasifier configuration

A schematic of the fluidized bed gasifier is shown in Fig. 4. Inconel 625 is a nickel-chromium alloy preferred over stainless steel 316 as the material of construction as it has excellent corrosion and heat resistance properties.

The outputs from the reactor design process are the gasifier diameter, height of the fluidized bed reactor and the distributor plate configuration. The reactor dimensions evaluated in the

design process are listed in Table 4. As shown in Fig. 4, the freeboard is kept b than the bed area size to reduce solid entrainment from the gasifier and to provide a longer residence time of the product gas to enhance tar cracking⁴⁷. The freeboard of the reactor is expanded up to a diameter of 0.19 m with a height of 0.3 m.

The location of feeding the biomass into the gasifier is an important criterion. It is beneficial for large systems to feed the biomass at the bottom, nearer to the distributor plate. This type of design is recommended to reduce tar and char content⁴⁸. In the present study, the feed-in point is 0.20 m above the distributor plate. The fluidized bed mainly comprises-of three parts: i) region below the distributor plate, called the plenum, ii) the main bed region above the distributor plate and iii) the top expanded zone is known i.e. freeboard. The main bed section is the section where the bed material is fluidized and the entire gasification reactions take place. This region also contains the biomass feed-in point. The main gasifier is equipped with three internal temperature indicators (TI) to monitor temperature at 1) just below the distributor plate and 0.1 m from the bottom of the gasifier, 2) located in the bed and 0.85 m from the bottom of the gasifier, and 3) situated in the freeboard and 1.85 m from the bottom section. The pressure differential indicator is provided between the point below the distributor plate and in the freeboard section to monitor the total pressure drop across the reactor. The additional air inlet is provided to ensure post-experiment combustion to remove any unwanted carbon in the gasifier and downstream. Similarly, N₂ is used to purge the gasification system to remove entrapped gases before the start of each experiment.

3.2 Gasifier operation

3.2.1 Temperature and pressure profiles

The fluidized bed gasifier as designed, built and described in this paper, is equipped with three internal TIs at different locations as shown in Fig. 4. Temperature variation at these points

needs to be monitored to avoid large variation of temperature within the reactor. Temperature variation in the bed is studied at three different temperature levels i.e. 600, 675 and 750°C. Temperature profiles are plotted with respect to time for 60 min, the total time of gasification considered for all of the experiments in the present study. Each temperature reading is taken at 6 min intervals.

Fig. 5 shows the temperature profiles in the bed (TI (2)) for the temperature of 600, 675 and 750°C over 60 minutes. The analysis shows no significant temperature variation in the bed for the ICA steam gasification system. Standard variations of the temperature readings are $\pm 5.0^\circ\text{C}$, $\pm 5.8^\circ\text{C}$ and $\pm 6.0^\circ\text{C}$ for 600°C, 675°C and 750°C, respectively. Thus, the variation is small, (<1%) and this is due to the carbonation reaction, an exothermic reaction, which produces heat for the endothermic gasification reactions. Similar observations are reported by other researchers⁴⁹ as well.

The temperature profiles at the three different locations in the fluidized bed gasifier can be seen in Fig. 6. The data shows the average value over 60 min. Attempts are made to keep the temperature constant throughout the fluidized bed reactor by using an external heating system. Amongst the three locations, significant variation is observed just below the distributor plate particularly at high temperature (675°C and 750°C) due to the steam injection at a lower temperature (250-300°C). The results show no significant variation in the freeboard temperature over the considered range for each experiment.

Initially, the pressure drop variation is measured with respect to time for each velocity i.e. 0.15 ($3U_{mf}$), 0.21 ($4U_{mf}$) and 0.26 m/s ($5U_{mf}$). A velocity to pressure drop diagram is then generated at a given fluidization velocity. The average pressure drop during 60 min gasification operation is then plotted with respect to fluidization velocity. The pressure drop is measured through the

pressure differential indicator (PDI) between the points located below the distributor plate and the freeboard region, as shown in Fig. 4.

Fig. 7 shows the pressure drop fluctuation with respect to time for different fluidization velocities i.e. 0.15, 0.21 and 0.26 m/s which represent 3, 4 and 5 times the fluidization velocity in the fluidized bed gasifier. The pressure drop evaluated using Equation (14) is shown for comparison (dotted line) which is based on the diameter to height ratio of 1.0. The analysis shows that total pressure drop increases as the fluidization velocities increases. The maximum pressure drop is observed at high fluidization velocity. However, low fluidization velocity produces a lower pressure drop and shows less fluctuation as compared to high fluidization velocities i.e. 0.21 m/s and 0.26 m/s.

Fig. 8 shows the relationship of pressure drop to fluidization velocity in the fluidized bed gasifier. The pressure drop represents an average value over 60 min of operational time. The analysis shows that the average pressure drop observed is in the range of 100-130 mbar by varying fluidization velocity in the range of 0.15-0.26 m/s. It shows that the pressure drop variation in the present study is not significant by varying the fluidization velocity between 0.15-0.26 m/s for the ICA steam gasification system. The bed starts to expand at the onset of minimum fluidization velocity, and a further increase in fluidization velocity does not show any significant increase in the pressure drop.

3.3 Gasifier operational challenges and solution

The following section elaborates operational problems observed in ICA steam gasification utilizing PKS as the feedstock. It also highlights the appropriate remedy for the associated problems related to the gasification system.

3.3.1 Downstream Clogging

The product gas carries tar (high hydrocarbon), excess steam, fine char and solid particles separated from the bed material due to attrition. The drastic decrease in temperature results in steam saturation and tar condensation in the mixture. In this situation, fine particles are started to agglomerate and produce a paste-like mixture which clogged the downstream pipe and equipment as shown in Fig. 9. Heating tape is used to provide a maximum temperature of 300-400°C to eliminate this effect. But due to the excess amount of steam in the product gas, the heating tape is not able to maintain sufficient heat at further distances along the pipe.

3.3.2 Presence of moisture in gas analyzing system

In the gas analyzing system, the product gas passes through the small condenser which separates the remaining moisture from the product gas stream. The efficiency of the condenser depends on the moisture present in the product gas. At high steam to biomass ratios, a high amount of unreacted steam exits from the gasifier and contributes a major part of the product gas stream. The product gas still carries a significant amount of moisture after passing through the cleaning system. Such high moisture level reduces—the separation efficiency of the condenser. The moisture enters into the tubing system of the analyzers, as shown in Fig. 10 (a) and then passes through the sample flow meter as shown in Fig. 10 (b) associated with the gas analyzing system. This situation results in the accumulation of moisture in the gas analyzing system which causes inaccurate measurements and serious damage to the gas analysing system.

3.3.3 Solutions to address operational problems

To avoid clogging in downstream, nitrogen is injected into the system just before the biomass feeding into the system. Nitrogen flows consume heat from the reactor at high temperature i.e. 600-750°C and then passed through, and heated up the pipe and equipment downstream. This enhanced the efficiency of the heating tape which is able to maintain high temperature operation between 300-400°C. This procedure is followed for all of the experiments to avoid

blockage within the system. The second problem is associated with moisture content and its presence in the gas analyzing system which can cause false readings of the product gas composition measured by the GC. This effect is eliminated by nitrogen purging before the start of each experiment. N₂ carried away any residual moisture and entrapped gases (H₂, CO, CO₂ and CH₄) present in the gas analyzing the system. N₂ purging is also used for a couple of minutes during the experiments for removal of the moisture. During this operation, the connection to the main analyzer is opened and the moisture is drained before entering the gas analyzer.

3.4 Performance of ICA gasification system

A few parameters are selected to identify the performance of the ICA gasification system in the context of the present work. However, the detailed experimental results and their optimization can be found elsewhere ^{13, 14, 19}.

Table 5 shows the product gas composition, hydrogen yield and gas heating values at 600, 675 and 750°C. The results infer that the H₂ composition (82.10 vol%) is maximum at 675°C while the CO₂ composition is zero at 600 and 675°C. However, at 750°C, the H₂ composition is drastically decreased to its minimum value (67.40 vol%) whereas CO₂ increases to its maximum value (7.57 vol%). This increase clearly shows the existence of reverse carbonation (calcination reaction) in the system which has been reported by Xu et al. ¹⁵ and Pfeifer et al. ¹⁶ at temperatures higher than 727°C and 675°C, respectively. Moreover, Zamboni et al. ¹⁷ and Aarlien et al. ¹⁸ reported maximum CO₂ sorption temperature at 660°C and 700°C for enhanced H₂ production, respectively. This infers the optimum temperature of 675°C is suitable for high H₂ composition with minimal CO₂ in ICA steam gasification and also provides evidence of a good fluidized bed operation in the present study. The lowest CH₄ concentration at 750 °C is due to high reactive steam methane reforming in the presence of the Ni catalyst which is further

verified by the highest CO concentration observed at 750 °C. The high activity of Ni catalyst in steam methane reforming at a temperature >740°C is also reported by other researchers ⁵⁰. It is concluded from the product gas profile of the ICA gasification system that the carbonation reaction remains effective at a lower temperature (600-675 °C, below the calcination temperature of CaCO₃) with high H₂ and negligible CO₂ content; while with higher temperature (750 °C) the process is dominated by Ni-based catalysed steam methane reforming, and generated high CO and low CH₄ concentrations. For this reason, the product gas profiles generated in ICA steam gasification might be different from biomass steam gasification with in-situ CO₂ adsorbent ²⁰ and biomass steam gasification using Ni catalyst ^{50, 51}. Besides, H₂ yield increases with increasing temperature and maximum yield (150.99 g H₂/kg biomass) is achieved at 750°C which is 5 times the yield at 600°C. The maximum H₂ yield at higher temperature is mainly due to the endothermic reactions of catalytic steam methane reforming and tar cracking ⁵² in the process. A comparative study of the ICA gasification system ((150.99 g H₂/kg biomass at 750 °C) with catalytic sorption enhanced steam gasification (133 g H₂/kg biomass at 700 °C in 0.5 g sample fixed bed reactor) ⁵³ shows the prospects of the present work. The lower heating values of the product show a continuous decrease as the temperature increases. This trend can be explained by decreasing trend of CH₄ with increasing temperature. Overall, the ICA steam gasification produces a gaseous mixture with medium heating values (12-18 MJ/Nm³). Besides, carbon conversion and gasification efficiency show an increasing trend as temperature increases. Low efficiencies at low temperature (600-675 °C) might be a case of negligible CO₂ and low activity of endothermic reactions.

The important aspect of the ICA steam gasification process is to maximize hydrogen generation in the product gas at lower gasification temperature. However, lower temperature in steam gasification might need to be observed closely due to high tar content nature of the process (as

shown in the Fig. 9). The proper heating of the downstream pipes and equipment needs to be maintained above tar condensation temperature up to the point of separation/collection.

4. Conclusions

The design considerations and pilot plant experiences of a bubbling fluidized bed gasification with integrated Ni catalyst and CO₂ adsorbent for enhanced are presented. The gasifier operation showed minimal temperature variation (< 1%) below distributor plate, in the bed, and freeboard regions. Similarly, minimal pressure drop (<150 mbar) is observed which is found proportional to fluidization velocities in the bed. The negligible CO₂ and high H₂ concentration (82 vol. %) in the product gas verify the active nature of the carbonation reaction even at a lower gasification temperature (600-675 °C, below the calcination temperature of CaCO₃). Moreover, high H₂ yield (31-150 g/kg biomass) and gas heating values (12.88-14.27 MJ/Nm³) at a temperature range of 600-750°C shows the good operation of the system. In order to address the issue of clogginer, nitrogen is injected into the system just before the biomass feeding system since N₂ flow may consume heat from the reactor at high temperature and could heat up the pipe and equipment downstream while passing through. For the solution of moisture accumulation, N₂ is purged before the start of each experiment since N₂ carried away any residual moisture and entrapped gases (H₂, CO, CO₂ and CH₄) present in the gas analyzing the system.

Acknowledgements

The authors greatly acknowledge the financial and technical support by University Teknologi PETRONAS. One of the authors would like to acknowledge the financial support provided by the Knowledge Foundation (KKS) of Sweden, Mälarenergi AB and Eskilstuna Energi och Miljö under the ‘PolyPO’ project.

References

1. Molino A, Chianese S and Musmarra D, Biomass gasification technology: The state of the art overview. *Journal of Energy Chemistry* **25**: 10-25 (2016).
2. Hossain MZ and Charpentier PA, 6 - Hydrogen production by gasification of biomass and opportunity fuels A2 - Subramani, Velu, in *Compendium of Hydrogen Energy*, ed by Basile A and Veziroğlu TN. Woodhead Publishing, Oxford, pp. 137-175 (2015).
3. Warnecke R, Gasification of biomass: comparison of fixed bed and fluidized bed gasifier. *Biomass and Bioenergy* **18**: 489-497 (2000).
4. McKendry P, Energy production from biomass (part 3): gasification technologies. *Bioresour Technol* **83**: 55-63 (2002).
5. Udomsirichakorn J and Salam PA, Review of hydrogen-enriched gas production from steam gasification of biomass: The prospect of CaO-based chemical looping gasification. *Renewable and Sustainable Energy Reviews* **30**: 565-579 (2014).
6. Yan L, He B, Pei X, Wang C, Duan Z, Song J and Li X, Design and comparisons of three biomass based hydrogen generation systems with chemical looping process. *International Journal of Hydrogen Energy* **39**: 17540-17553 (2014).
7. Cormos CC, Biomass direct chemical looping for hydrogen and power co-production: Process configuration, simulation, thermal integration and techno-economic assessment. *Fuel Processing Technology* **137**: 16-23 (2015).
8. Hafizi A, Rahimpour MR and Hassanajili S, High purity hydrogen production via sorption enhanced chemical looping reforming: Application of $22\text{Fe}_2\text{O}_3/\text{MgAl}_2\text{O}_4$ and $22\text{Fe}_2\text{O}_3/\text{Al}_2\text{O}_3$ as oxygen carriers and cerium promoted CaO as CO_2 sorbent. *Applied Energy* **169**: 629-641 (2016).
9. Dou B, Wang K, Jiang B, Song Y, Zhang C, Chen H and Xu Y, Fluidized-bed gasification combined continuous sorption-enhanced steam reforming system to continuous hydrogen production from waste plastic. *International Journal of Hydrogen Energy* **41**: 3803-3810 (2016).

10. Kumagai S, Alvarez J, Blanco PH, Wu C, Yoshioka T, Olazar M and Williams PT, Novel Ni–Mg–Al–Ca catalyst for enhanced hydrogen production for the pyrolysis–gasification of a biomass/plastic mixture. *J Anal Appl Pyrolysis* **113**: 15-21 (2015).
11. Huang B-S, Chen H-Y, Chuang K-H, Yang R-X and Wey M-Y, Hydrogen production by biomass gasification in a fluidized-bed reactor promoted by an Fe/CaO catalyst. *Int J Hydrogen Energy* **37**: 6511-6518 (2012).
12. Udomchoke T, Wongsakulphasatch S, Kiatkittipong W, Arpornwichanop A, Khaodee W, Powell J, Gong J and Assabumrungrat S, Performance evaluation of sorption enhanced chemical-looping reforming for hydrogen production from biomass with modification of catalyst and sorbent regeneration. *Chem Eng J* **303**: 338-347 (2016).
13. Khan Z, Yusup S, Ahmad MM and Chin BLF, Hydrogen production from palm kernel shell via integrated catalytic adsorption (ICA) steam gasification. *Energy Conversion and Management* **87**: 1224-1230 (2014).
14. Yusup S, Khan Z, Ahmad MM and Rashidi NA, Optimization of hydrogen production in in-situ catalytic adsorption (ICA) steam gasification based on Response Surface Methodology. *Biomass and Bioenergy* **60**: 98-107 (2014).
15. Xu G, Murakami T, Suda T, Kusama S and Fujimori T, Distinctive effects of CaO additive on atmospheric gasification of biomass at different temperatures. *Ind Eng Chem Res* **44**: 5864-5868 (2005).
16. Pfeifer C, B. Puchner and Hofbauer H, In-situ CO₂-absorption in a dual fluidized bed biomass steam gasifier to produce a hydrogen rich syngas. *International Journal of Chemical Reactor Engineering* **5**, **A9**: 1-13 (2008).
17. Zamboni I, Debal M, Matt M, Girods P, Kiennemann A, Rogaume Y and Courson C, Catalytic gasification of biomass (*Miscanthus*) enhanced by CO₂ sorption. *Environmental Science and Pollution Research*: 1-14 (2016).
18. Aarlien R, Røkke NA, Svendsen HF, Schweitzer D, Beirow M, Gredinger A, Armbrust N, Waizmann G, Dieter H and Scheffknecht G, Pilot-scale demonstration of Oxy-SER steam

- gasification: production of syngas with pre-combustion CO₂ capture. *Energy Procedia* **86**: 56-68 (2016).
19. Khan Z, Yusup S, Ahmad MM and Rashidi NA, Integrated catalytic adsorption (ICA) steam gasification system for enhanced hydrogen production using palm kernel shell. *Int J Hydrogen Energy* **39**: 3286-3293 (2014).
 20. Han L, Wang Q, Yang Y, Yu C, Fang M and Luo Z, Hydrogen production via CaO sorption enhanced anaerobic gasification of sawdust in a bubbling fluidized bed. *Int J Hydrogen Energy* **36**: 4820-4829 (2011).
 21. Hambali E and Rivai M, The Potential of Palm Oil Waste Biomass in Indonesia in 2020 and 2030. *IOP Conference Series: Earth and Environmental Science* **65**: 012050 (2017).
 22. National Biomass Strategy 2020: New wealth creation for Malaysia's palm oil industry (2011).
 23. Garcia-Nunez JA, Ramirez-Contreras NE, Rodriguez DT, Silva-Lora E, Frear CS, Stockle C and Garcia-Perez M, Evolution of palm oil mills into bio-refineries: Literature review on current and potential uses of residual biomass and effluents. *Resources, Conservation and Recycling* **110**: 99-114 (2016).
 24. Abdullah SS and Yusup S, Method for screening of Malaysian biomass based on aggregated matrix for hydrogen production through gasification. *Journal of Applied Sciences* **10**: 3301-3306 (2010).
 25. Leung DYC, Caramanna G and Maroto-Valer MM, An overview of current status of carbon dioxide capture and storage technologies. *Renewable and Sustainable Energy Reviews* **39**: 426-443 (2014).
 26. Florin NH and Harris AT, Enhanced hydrogen production from biomass with in situ carbon dioxide capture using calcium oxide sorbents. *Chem Eng Sci* **63**: 287-316 (2008).
 27. Florin NH and Harris AT, Hydrogen production from biomass coupled with carbon dioxide capture: The implications of thermodynamic equilibrium. *Int J Hydrogen Energy* **32**: 4119-4134 (2007).

28. Tsai W-T, Hsien K-J, Hsu H-C, Lin C-M, Lin K-Y and Chiu C-H, Utilization of ground eggshell waste as an adsorbent for the removal of dyes from aqueous solution. *Bioresour Technol* **99**: 1623-1629 (2008).
29. Mustakimah M., Suzana Y. and Saikat M., Decomposition study of Calcium Carbonate in Cockle Shell, in World Engineering Congress: Conference on Engineering and Technology Education, Kuching, Sarawak, Malaysia pp. 16-22 (2-5 August, 2010).
30. Khan Z, Yusup S, Ahmad MM and Chin BLF, Performance study of Ni catalyst with quicklime (CaO) as CO₂ adsorbent in palm kernel shell steam gasification for hydrogen production. *Advanced Materials Research* **917**: 292-300 (2014).
31. Gil J, Corella J, Aznar MP and Caballero MA, Biomass gasification in atmospheric and bubbling fluidized bed: Effect of the type of gasifying agent on the product distribution. *Biomass and Bioenergy* **17**: 389-403 (1999).
32. Chan FL and Tanksale A, Review of recent developments in Ni-based catalysts for biomass gasification. *Renewable and Sustainable Energy Reviews* **38**: 428-438 (2014).
33. Sutton D, Kelleher B and Ross JRH, Review of literature on catalysts for biomass gasification. *Fuel Processing Technology* **73**: 155-173 (2001).
34. Basu P, Combustion and Gasification in Fluidized Beds. CRC Press (2006).
35. R. H. Perry and Green DW, Perry's Chemical Engineering's Handbook. McGraw Hill, pp. 2-309 (1999).
36. Cooper JR, The International Association for the Properties of Water and Steam (2007).
37. D. Kunii and Levenspiel O, Fluidization Engineering Butterworth-Heinemann (1992).
38. Rhodes M, Introduction to particle technology John Wiley and Sons (1998).
39. Weerachanchai P, Horio M and Tangsathitkulchai C, Effects of gasifying conditions and bed materials on fluidized bed steam gasification of wood biomass. *Bioresour Technol* **100**: 1419-1427 (2009).
40. Basu P, Combustion and gasification in fluidized bed. Taylor and Francis (2006).
41. Kaushal P, Abedi J and Mahinpey N, A comprehensive mathematical model for biomass gasification in a bubbling fluidized bed reactor. *Fuel* **89**: 3650-3661 (2010).

42. Nikoo MB and Mahinpey N, Simulation of biomass gasification in fluidized bed reactor using ASPEN PLUS. *Biomass and Bioenergy* **32**: 1245-1254 (2008).
43. Gordillo ED and Belghit A, A two phase model of high temperature steam-only gasification of biomass char in bubbling fluidized bed reactors using nuclear heat. *Int J Hydrogen Energy* **36**: 374-381 (2011).
44. Horio M and Nonaka A, A generalized bubble diameter correlation for gas-solid fluidized beds. *AIChE Journal* **33**: 1865-1872 (1987).
45. Yang WC, Handbook of Fluidization and Fluid-Particle Systems. Taylor & Francis (2003).
46. Qureshi AE and Creasy DE, Fluidised bed gas distributors. *Powder Technology* **22**: 113-119 (1979).
47. van den Enden PJ and Lora ES, Design approach for a biomass fed fluidized bed gasifier using the simulation software CSFB. *Biomass and Bioenergy* **26**: 281-287 (2004).
48. Corella J, Aznar MP, Delgado J and Aldea E, Steam gasification of cellulosic wastes in a fluidized bed with downstream vessels. *Industrial & Engineering Chemistry Research* **30**: 2252-2262 (1991).
49. Acharya B, Dutta A and Basu P, Chemical-looping gasification of biomass for hydrogen-enriched gas production with in-process carbon dioxide capture. *Energy & Fuels* **23**: 5077-5083 (2009).
50. Li J, Yin Y, Zhang X, Liu J and Yan R, Hydrogen-rich gas production by steam gasification of palm oil wastes over supported tri-metallic catalyst. *Int J Hydrogen Energy* **34**: 9108-9115 (2009).
51. Dong L, Wu C, Ling H, Shi J, Williams PT and Huang J, Development of Fe-promoted Ni–Al catalysts for hydrogen production from gasification of wood sawdust. *Energy & Fuels* **31**: 2118-2127 (2017).
52. Mahishi MR and Goswami DY, An experimental study of hydrogen production by gasification of biomass in the presence of a CO₂ sorbent. *Int J Hydrogen Energy* **32**: 2803-2808 (2007).

53. Zhang Y, Gong X, Zhang B, Liu W and Xu M, Potassium catalytic hydrogen production in sorption enhanced gasification of biomass with steam. *Int J Hydrogen Energy* **39**: 4234-4243 (2014).

Tables

Table 1. Proximate and ultimate analysis of PKS²⁴

Moisture	(wt %)	9.61
Proximate analysis	(wt. % dry basis)	
Volatile matter		81.03
Fixed carbon		14.87
Ash content		4.10
Ultimate analysis	(wt. % dry basis)	
C		49.65
H		6.13
N		0.41
S		0.48
O (by difference)		43.33
Higher heating value	(MJ/kg)	20.40

Table 2. Physical properties and chemical composition of CaO (bed material)³⁰ and steam^{35 36}

Bed Material (CaO)		
Particle density	[kg/m ³]	3053
Bulk density	[kg/m ³]	1047
Chemical composition	(wt. %)	
CaO		93.32
MgO		4.24
SiO ₂		0.95
Fe ₂ O ₃		0.23
Other metal oxides (MnO, CuO, SrO, ZnO)		1.0
Steam (At 750 °C, 1 atm)		
Density (kg/m ³)		0.22
Viscosity (Pas)		4×10 ⁻⁵

Table 3. Input design parameter for distributor plate design

Orifice diameter	(m)	0.002
Minimum fluidization velocity	[m/s]	0.051
Gas (steam) superficial velocity	[m/s]	0.26
Bed voidage	-	0.66
D/Z	-	1.0
R_c	-	0.089

Table 4. Fluidized bed gasifier system configuration

Internal diameter (ID)	[m]	0.15
Total height	[m]	2.00
Freeboard height	[m]	0.30
Freeboard ID	[m]	0.19
Plenum height	[m]	0.30
Distributor plate hole ID	[m]	0.002
Feeding point location from the distributor	-	0.20
Number of orifices in the distribution plate	-	158
Operating temperature	[°C]	600-750
Preheat temperature of the steam	[°C]	250-300

Table 5. Effect of temperature on performance parameters

Temperature	[°C]	600	675	750
Biomass feed rate	[kg/h]	1.35	1.35	1.35
Steam/biomass	[wt/wt]	2.0	2.0	2.0
Adsorbent to biomass	[wt/wt]	1.0	1.0	1.0
Catalyst to biomass ratio	[wt/wt]	0.1	0.1	0.1
Gas composition (dry-N ₂ free)	[vol%]			
H ₂		78.00	82.10	67.40
CO		8.78	6.45	14.33
CO ₂		0.00	0.00	7.57
CH ₄		13.22	11.43	10.70
Hydrogen yield	[g/kg biomass]	31.80	80.39	150.99
Lower heating value	[MJ/Nm ³]	14.27	13.78	12.88
Carbon conversion efficiency	[%]	11.06	20.06	87.01